

## CHAPTER 1

# REAL TIME MONITORING OF NEUROMODULATORS IN BEHAVING ANIMALS USING GENETICALLY ENCODED INDICATORS

Grace O. Mizuno\*, Elizabeth K. Unger\* and Lin Tian<sup>†</sup>

\*Department of Biochemistry and Molecular Medicine,  
School of Medicine, University of California, Davis, USA

<sup>†</sup>lintian@ucdavis.edu

---

### 1.1 Introduction

Behavior is driven by precise spatial and temporal patterns of neural activity. Understanding how the brain processes these complex patterns requires large-scale recording and manipulation of genetically defined neuronal populations in behaving animals. Over the past decade, protein engineering has produced high-quality genetically encoded indicators to detect changes in calcium, voltage, fast neurotransmitters (glutamate/GABA), and vesicular release. In combination with modern microscopy techniques, these sensors, especially genetically encoded calcium indicators (GECIs), have enabled large-scale recordings from genetically defined neurons or glial cells with cellular and sub-cellular resolution. In addition, sensors with non-overlapping spectra now enable multiplexed imaging of calcium and voltage or can be combined with optogenetic manipulations. These advances provide new opportunities for *in vivo* dissection of cellular and circuit activity and its relationship to behavior.

---

\*Equal contribution.

Much of the focus of neuroscience has been on the rapid inputs and outputs of neurons, however the immense importance of neuromodulators in profoundly influencing neuronal and astrocytic function is now coming to light. The functional significance of their ability to modulate global brain processes such as arousal, attention, or emotion is now well recognized. Yet how they control the activity of local neurons in the brain — how they alter circuit dynamics or modulate behavioral states — is largely unknown. Analytical chemistry has provided useful insights about the concentrations of neuromodulators in the brain via *in situ* microdialysis, fast scan cyclic voltammetry (FSCV), and amperometry with enzyme-modified electrochemical sensors; however, these methods face limitations that prevent large-scale measurements of neuromodulator release in behaving animals.

To address these technical barriers, we and other labs have developed a toolbox of genetically encoded indicators that enable direct, specific and long-term imaging of neuromodulatory signals in target circuits during natural behavior. dLight1, provides high molecular specificity, rapid temporal response (10 ms on and 100 ms off), cellular-level spatial resolution, and stable, long-term measurements over hours, days, or even months. Applications of dLight1 have started to lead to new discoveries about the neural mechanisms controlling dopamine release.

Here we focus on recent developments and applications of genetically encoded indicators for neurotransmitters and neuromodulators. We take an in-depth look at the design and screening of these sensors based on various protein scaffolds. We also discuss the novel applications these new optical probes have enabled, as well as practical concerns in awake, behaving animals. In combination with calcium/voltage imaging and optogenetics, the fast-growing toolbox of sensors for chemical transmission is well-poised to permit direct functional analysis of how the spatiotemporal coding of chemical input signaling mediates the plasticity and function of brain circuits.

## 1.2 Design of genetically encoded indicators of neural activity

Recent advances in the creation and optimization of genetically encoded (i.e. protein-based) sensors for a variety of molecules and cellular states have led to several high-quality optical probes, such as the genetically encoded calcium indicator (GCaMP) family of GECIs and voltage sensors based on either opsins or voltage sensing domains. Meanwhile, advances in the speed, depth of penetration, and spatial resolution of fluorescence microscopy techniques have extended our ability to non-invasively measure neural activity with superior spatiotemporal resolution. Combined with advanced microscopy, calcium imaging using GCaMPs is now routinely employed to enable large-scale, mesoscopic recording of neuronal

populations or glia cells at 30 Hz or faster and with subcellular resolution in awake, behaving animals.

Protein-based sensors typically consist of an analyte-binding or sensing domain and a reporter element based on either a single fluorescence protein (FP) or two FPs. In the case of two FP-based sensors, the FPs have overlapping excitation and emission spectra. The conformational changes in the analyte-binding or sensing domain move the two FPs into sufficient proximity for Förster Resonance Energy Transfer (FRET) between the two FPs to occur, and the readout is a ratio of the intensities of the two FPs. In the case of single FP sensors, changes in the cellular environment detected by the analyte binding or sensing domain result in changes in the chromophore environment of the FP leading to an increase or decrease in fluorescence intensity. Single FP based indicators offer several appealing advantages, such as superior sensitivity, enhanced photostability, broader dynamic range, and faster kinetics compared to FRET-based indicators (Piston and Kremers, 2007). They are also relatively small, and thus easier to express in an adeno-associated virus (AAV) and to target to subcellular locations, such as spines and axon terminals. In addition, imaging with single-FP indicators preserves spectrum bandwidth, thus allowing for multiplexed imaging or use alongside optogenetic effectors, such as channelrhodopsin.

The main advantage of these sensors over small molecule-based fluorophores stems from their genetic encoding, which enables reporters to be constructed from proteins that are evolutionarily designed to respond to neural activity. This enables them to be optimized by computational modeling and directed evolution. Then they can be selectively targeted to cells with specific anatomical connectivity. Finally, these sensors can be stably expressed over long periods of time (from days to months), allowing neuroscientists to study how patterns of neural activity change with learning, development, or disease progression. *For reviews please see (Palmer et al., 2011; Broussard et al., 2014a; Lin and Schnitzer, 2016).*

In recognition of the potential of combining genetically encoded indicators with modern microscopy, we and others have now extended the concept of single-FP based sensors to the design of genetically encoded sensors for neurotransmitters and neuromodulators. Genetically encoded indicators are generally categorized by their scaffold: G-protein coupled receptors (GPCR) and bacterial periplasmic binding proteins (PBP).

### 1.3 dLight1: A GPCR-based dopamine indicator

To enable direct and specific measurements of diverse types of neuromodulators with the necessary spatiotemporal resolution, it is advantageous to design a sensor with molecular specificity, affinity, and kinetics similar to endogenous receptors.

As GPCRs are native neuromodulator targets, we have pioneered a new approach for biosensor design based on protein engineering of the cognate GPCRs. This approach, facilitated by recent advances in GPCR structural biology, allows us to leverage the ligand specificity, affinity, and binding kinetics that has evolved in the GPCR family and provides a universal platform to design sensors for any desired neuromodulator or pharmacological drug. Using this design platform, we engineered dLight1, a suite of intensity-based genetically encoded indicators for dopamine (DA) that work by directly coupling the conformational changes of inert human dopamine receptors to changes in the fluorescence intensity of a circularly permuted GFP (cpGFP) (Patriarchi *et al.*, 2018). The dLight1 family consists of six sensors based on three dopamine receptors (DRD1, DRD2, and DRD4) with broadly tunable affinity and dynamic range to probe dopamine transients across the pM–mM range of concentrations. We have also applied the design strategy of dLight1 to develop a class of intensity-based sensors for serotonin, norepinephrine, melatonin and opioid peptides. Below we use dLight1 as a prototype to discuss GPCR-based sensor design, characterization and applications.

### 1.3.1 Sensor engineering and screening pipeline

To engineer a GPCR-based sensor, the optimal insertion site of cpGFP first needs to be determined. The ideal insertion site in a GPCR would maximize the coupling of fluorescence changes with conformational changes of the receptor upon ligand binding without interfering with membrane trafficking. Crystallography has yielded detailed structural information on both the active and inactive states of  $\beta_2$  adrenergic receptor ( $\beta_2$ AR), a catecholamine receptor, which suggested that intracellular loop 3 (IL3) undergoes significant conformational change upon ligand binding. Given the structural similarity of GPCRs, it was hypothesized that insertion of cpGFP into IL3 of DRDs would alter the chromophore environment of cpGFP resulting in a change in cpGFP fluorescence. To determine the insertion site of cpGFP, DRD1 and DRD4 were first aligned with that of  $\beta_2$ AR. The exact site of the cpGFP insertion into IL3 was further optimized based on expression on the membrane. The cpGFP module (LSSLE-cpGFP-LPDQL) from GCaMP was inserted between K232 and K269 of DRD1 (Patriarchi *et al.*, 2018). When expressed in human embryonic kidney cells (HEK), this mutant was well-expressed at the plasma membrane. However, when DA was applied, we observed a decreased fluorescence signal at the cell membrane.

Through engineering GCaMP (Tian *et al.*, 2009) and the glutamate sensing fluorescent reporter, iGluSnFR (Marvin *et al.*, 2013), we learned that both linker regions between the ligand-binding proteins and cpGFP are critical for a sensor's dynamics and kinetics. Therefore, to further optimize and obtain a positive-response

sensor, a linker library on each side of the cpGFP (LSSXX-cpGFP-XXDQL) was engineered and variants were screened for their responses in mammalian HEK cells. After screening a library of 585 variants in HEK cells and tuning the dynamic range with mutations in IL3 we obtained a suite of dLight1 sensors with excellent membrane localization and varying dynamic ranges (~100% to 1000%  $\Delta F/F$ ) and affinities to cover a broad range of physiologically relevant concentrations (pM to mM) (Patriarchi *et al.*, 2018).

### 1.3.2 Sensor characterization: Affinity, specificity, and kinetics

Before applying sensors *in vivo*, it is important to perform systematic characterization of the sensor's intrinsic properties, including affinity, specificity, and kinetics. We used *in situ* ligand titration in HEK cells to determine the apparent affinity and molecular specificity of the sensor (Patriarchi *et al.*, 2018). The apparent affinity combined with the dynamic range of a sensor can be used to predict the sensitivity to physiologically relevant release, thus guiding the selection of sensors for *in vivo* applications. The apparent affinities and dynamic ranges of the dLight1 family based on various DRDs are shown in Table 1.1.

For monoamines, it is critical to confirm ligand specificity as they are structurally very similar. While DA and norepinephrine (NE) only differ by one hydroxyl group, their affinities for dLight1.1 (based off DRD1) are vastly different: the  $K_d$  of dLight1.1(DRD1 based sensor) for DA is 330 nM while the  $K_d$  of dLight1.1 for NE is 19,850 nM, which is a 40 fold lower affinity (Patriarchi *et al.*, 2018). Negligible responses were observed for other neurotransmitters and neuromodulators, including epinephrine, octopamine, serotonin, GABA, histamine, and acetylcholine.

One of the major concerns using an endogenously expressed receptor as a sensor is the possibility of endogenous signaling interference. To investigate this, the effect of the sensor expression on ligand-induced cyclic AMP (cAMP) production was monitored. dLight1.1 did not display significant cAMP response in HEK cells. Furthermore, when dLight1.1 was introduced into U2OS, a cell line that endogenously expresses DRD1, dLight1.1 did not significantly alter the DA dose-response curve (Patriarchi *et al.*, 2018).

Next, dLight1.1 was characterized in primary rat hippocampal neurons. To do so, the sensor was first cloned into an adeno-associated viral vector driven by a human synapsin or CAG promoter. Similar to in HEK cells, in primary rat hippocampal neurons, dLight1.1 showed excellent membrane localization and a similar affinity for DA ( $K_d$  311 nM) (Patriarchi *et al.*, 2018). In cultured hippocampal slices, dLight1.1 reliably detects sub-micromolar DA concentration changes at dendrites and single dendritic spines.

**Table 1.1** The apparent affinity and dynamic range of the dLight1 family.

Version	GPCR	Dynamic Range	Affinity
dLight1.1	DRD1	230 ± 9%	330 ± 30 nM
dLight1.2	DRD1	340 ± 20%	770 ± 10 nM
dLight1.3a	DRD1	660 ± 30%	2300 ± 20 nM
dLight1.3b	DRD1	930 ± 30%	1680 ± 10 nM
dLight1.4	DRD4	170 ± 10%	4.1 ± 0.2 nM
dLight1.5	DRD2	180 ± 10%	110 ± 10 nM

Lastly, we used dLight1.2 (based on DRD1 with additional mutations) to measure the time course of dopamine release triggered by electrical stimulation in acute striatal slices with two photon imaging (Patriarchi *et al.*, 2018). Fast line scan revealed a rapid onset of fluorescence increase (rise  $\tau_{1/2} = 9.5 \pm 1.1$  ms) followed by a plateaued peak (averaged  $\Delta F/F = 220 \pm 50\%$ ) for about 150 ms, which decayed to baseline in about 400 ms (decay  $\tau_{1/2} = 90 \pm 11$  ms). Blockade of dopamine reuptake with cocaine significantly prolonged the decay of fluorescence from peak to baseline, but with equivocal effect on response amplitude ( $P = 0.056$ ). Application of the competitive antagonist SKF83566 eliminated the responses, confirming that fluorescent signals are indeed due to DA binding.

1.3.3 Application of dLight1

dLight1 offers fast temporal resolution, matching that of electrochemical methods for detecting monoamines, while also providing subcellular resolution and molecular specificity. dLight1 enables the measurement of DA reuptake versus diffusion which would not be possible with other methods. These properties of dLight1 enable robust and chronic detection of physiologically or behaviorally relevant DA transients, which opens new doors to study how neuromodulators govern the rapid changes in activity and brain state.

One of the major questions surrounding DA is the concentration of DA release and its synaptic and extra-synaptic contribution to circuit function. By utilizing the fast kinetics of dLight1.2, we observed peak DA concentrations of 10–30  $\mu\text{M}$  in acute striatal slices following electrical stimulation: such concentrations were closely associated with sites of release (Patriarchi *et al.*, 2018). Under similar stimulus parameters, DA concentrations reported with FSCV are 1–2 orders of magnitude lower (Yorgason *et al.*, 2017).

dLight1 also permits deep-brain recording of bi-directional dopamine dynamics compatible with optogenetic stimulation or calcium imaging of local neuronal activity in freely behaving mice. dLight1.1, when used together with ChrimsonR (a red-shifted optogenetic actuator), reported an increase of DA in the nucleus accumbens (NAc) when optogenetically activating DAergic neurons in the ventral tegmental area (VTA) (Figure 1.1A) and a decrease of DA when inhibiting DAergic neurons through optogenetic stimulation of GABAergic neurons in the VTA (Figure 1.1B). Furthermore, when performing dual-color imaging, the fluorescence of dLight1.1 and red-shifted calcium indicator, jRGECO1a, increased while consuming sucrose. However, dLight1.1 fluorescence decreased while the fluorescence of red-shifted calcium indicator, jRGECO1a,

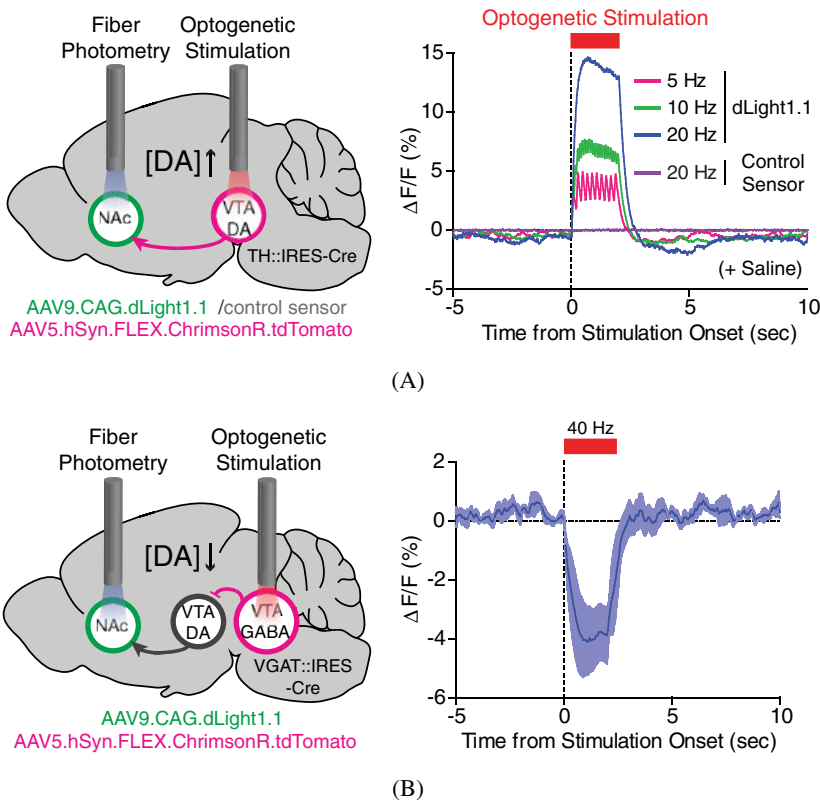


**Figure 1.1** (A) Schematics showing fiber photometry recording of dLight1.1 or control sensor in the NAc while stimulating VTA DA neurons by optogenetics. Averaged fluorescence increase in response to optogenetic stimuli ( $n = 5$  mice). (B) Schematics showing fiber photometry recording of dLight1.1 in the NAc and optogenetic stimulation of VTA GABA neurons that inhibits VTA DA neurons. Averaged fluorescence decrease in response to optogenetic stimulation at 40 Hz ( $n = 4$  mice). Figures reproduced with permission from Patriarchi *et al.*, 2018.

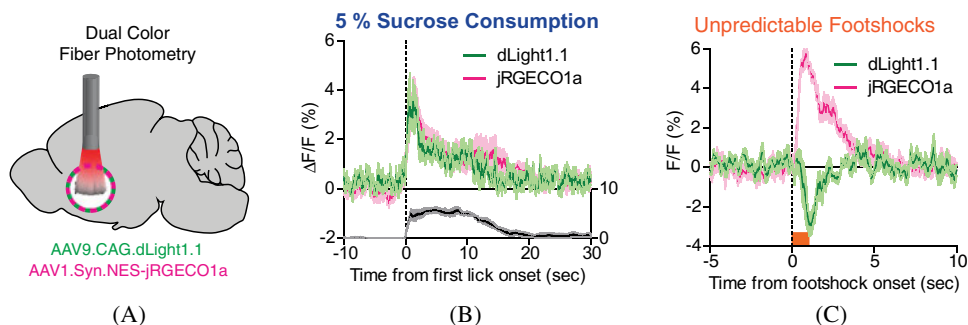


**Figure 1.2** (A) Dual-color fiber photometry recording of DA release with dLight1.1 and local neuronal activity with jRGECO1a. (B) Fluorescence increase or decrease in dLight1.1 (green) and increase in jRGECO1a (red) during unpredictable reward or (C) footshock delivery (0.6 mA for 1 s,  $n = 5$  mice). Figures reproduced with permission from Patriarchi *et al.*, 2018.

increased during unexpected footshock (Figure 1.2). These findings demonstrate dLight1 can be used with calcium imaging to correlate postsynaptic local circuit activity with DA input signals. We were also able to use dLight1.1 to chronically measure learning-induced dynamic changes of DA transients within the NAc at sub-second resolution. Mice trained using Pavlovian conditioning displayed an increase of DA response to predictive cues and a decrease to reward consumption (Figure 1.3).

As DA neurons are densely confined in relatively small deep-brain areas and extensively project to distant brain regions to modulate local circuitry, it is extremely important to analyze different spatiotemporal transients across depth. One of the most powerful aspects of genetically encoded sensors such as dLight1 is the ability to allow for imaging cellular activity at spatial scales ranging from subcellular to millimeter. Therefore, we performed two-photon imaging with dLight1.2 in layers 1 and 2 of mouse motor cortex, which revealed a high-resolution (cellular level) dopamine transient map of spatially distributed, functionally heterogeneous dopamine signals during a visuomotor learning task (Figure 1.4). Our results suggest that DA release from mesocortical projections are thus spatially intermingled and depends on motor behavior, reward expectation and consumption.

Dissemination of dLight1 to the neuroscience community has led to new discoveries involved in the neural mechanisms of DA release in modulating motivation, reinforcement, and rewarding and aversive stimuli. Using dLight1, the Lüscher lab demonstrated DA's direct involvement in the reinforcing effect of heroin, a hypothesis severely challenged largely based on pharmacological



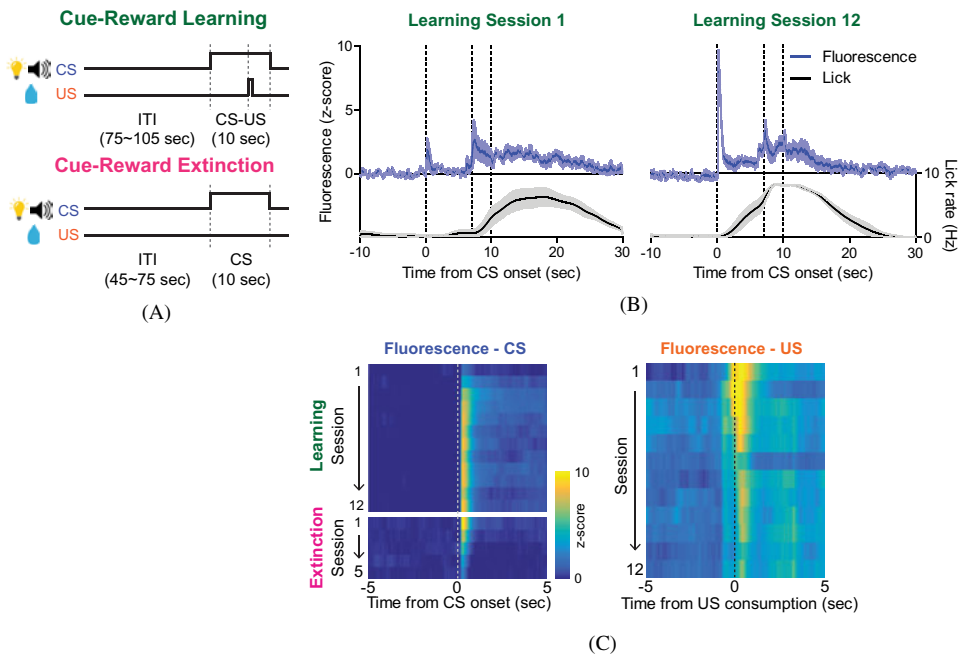


**Figure 1.3** (A) Pavlovian conditioning procedures involved learning to associate neutral cues (CS; house light and 5 kHz tone) with a sucrose reward (US; 50 $\mu$ L of 5% sucrose), and subsequent extinction. (B) dLight1.1 dynamics in response to CS and US in first and last sessions of cue-reward learning, shown in single (gray) and averaged (blue) trials (n=20 trials) from a single animal. (C) Evolution of CS- (left) and US-evoked (right panel) average fluorescence. Figures reproduced with permission from Patriarchi *et al.*, 2018.

experiments suggesting DA-independent mechanisms for heroin reinforcement (Corre *et al.*, 2018). Using fiber photometry dLight1.1 in the NAc medial shell resulted in an increase in fluorescence after self-administration of heroin during initial reinforcement within less than a minute through the activation of a subset of DAergic neurons in the medial VTA. The Lammel lab, on the other hand, used dLight1 combined with calcium imaging to reveal an anatomically and functionally distinct DA projection underlying motivated behavior (de Jong *et al.*, 2019). They discovered that DA terminals in the ventral NAc medial shell are excited by unexpected aversive outcomes and to cues that predict them, whereas excitation in response to reward-predictive cues dominated in the NAc lateral shell and was largely absent in the medial shell. Recording of direct and specific DA transients using dLight1 combined with calcium imaging make it possible to monitor functionally and anatomically distinct heterogeneous subpopulations of neurons important for a wide range of behaviors.

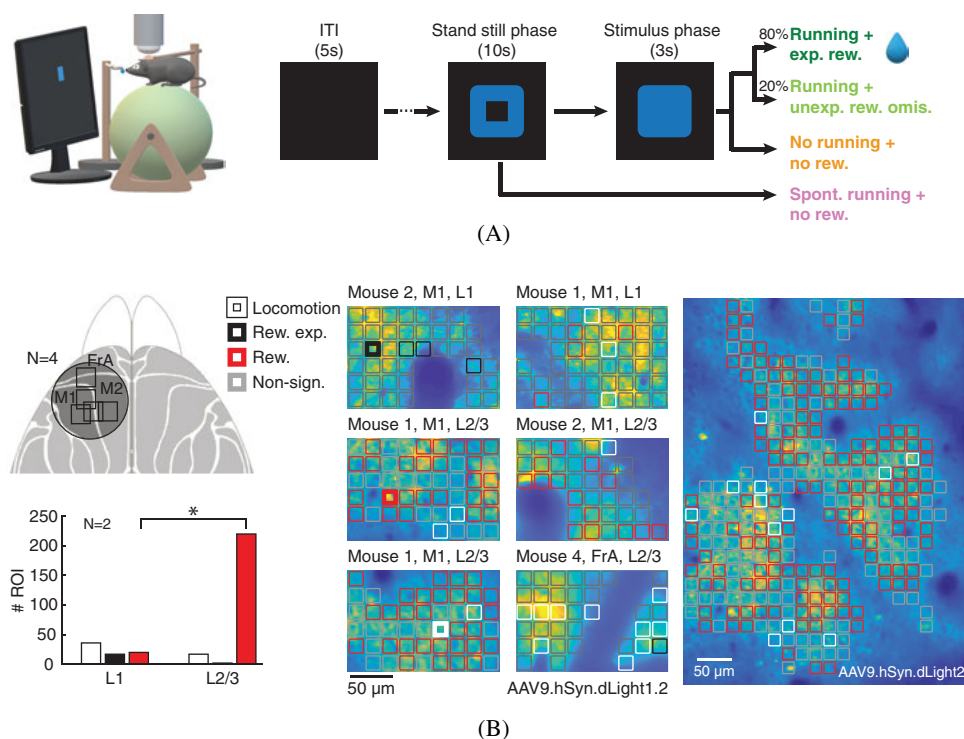


**Figure 1.4** Two-photon imaging revealed spatially-distinct, task specific DA transients in motor cortex. (A) Schematics of experimental setup. To initiate a trial, mice were required to stand still for 10s following a visual cue (blue square). If mice started to run during the stimulus phase (“Hit trials”), a water reward was given. In 20% of randomly selected “Hit trials” the reward was withheld. If no run was triggered by stimulus presentation, the trials were counted as “Miss trials”. Erroneous/spontaneous runs during the stand-still phase ended the trial (no “Go” cue or reward). (B) Dorsal view of mouse cortex with the chronic cranial window (circle) and imaging location indicated (square). Heatmap of dLight1.2 expression pattern in layer 2/3 of M1 cortex. The image is overlaid with computationally defined regions of interest (ROIs,  $\sim 17 \times 17 \mu\text{m}$ ). Colored ROIs indicate the type of fluorescence responses observed during the task. Figures reproduced with permission from Patriarchi *et al.*, 2018.

### 1.3.4 Scaffold versatility: Other neurotransmitters, neuromodulators and neuropeptides

The abundance of GPCRs for neurotransmitters and neuropeptides is advantageous from a sensor design point of view. We demonstrated the universality of applying the design strategy of dLight1 to develop a class of intensity-based sensors for various neurotransmitters, neuromodulators and neuropeptides, such as serotonin, norepinephrine, melatonin and opioid peptides (Patriarchi *et al.*, 2018). However, while all receptors share similar structural motifs, each sensor must be individually mutagenized and optimized.

## 1.4 From glutamate to neuromodulators: Bacterial PBP-based single-FP sensors: iMaltSnFR and iGluSnFR

The Looger lab has shown that bacterial PBPs can be converted into sensors *via* the insertion of cpGFP in loops tolerant of insertions, followed by significant direct evolution to discover mutants with desired intrinsic properties. PBPs consist of two lobes connected by a hinge region, which close around the ligand in a Venus flytrap-like motion (Dwyer and Hellenga, 2004). The first PBP based sensor was first developed from the *E. coli* maltodextrin-binding protein (MalE) (Marvin *et al.*, 2011). Using the crystal structures of the ligand-free (open) and the ligand-bound (closed) conformations, residues sensitive to ligand-dependent structural changes were identified. These residues were hypothesized to be well-suited for modulating the fluorescence of an inserted cpGFP. After sequential rounds of screening, iMaltSnFR was created that had a  $\Delta F/F$  of greater than 600%. iMaltSnFR was the foundation for the neurotransmitter sensor, iGluSnFR, which reports the presence of the excitatory molecule glutamate, based on the bacterial protein, GltI (Marvin *et al.*, 2013). iGluSnFR was developed by inserting cpGFP into GltI, which has significant homology to the glutamate-binding domain from ionotropic glutamate receptors. Although GltI had been previously used to develop FRET-based glutamate sensors, the single-FP based iGluSnFR, including versions recently optimized for their kinetics and affinities, are the first optical sensors with sufficient sensitivity and photostability to permit reliable *in vivo* optical measurements of glutamate transients in single dendritic spines (Helassa *et al.*, 2018; Marvin *et al.*, 2018).

iGluSnFR has been publicly available for many years now and several groups have used it to study glutamate release from neurons and glia in applications including the hippocampus, the cerebellum, the visual system, Huntington's disease, Rett syndrome, and many more. A wide range of model organisms were used for these studies, including iPSCs, flies, fish and mice. The Allen Institute has even created a mouse for conditional expression of iGluSnFR, which one lab used to do mesoscopic whole brain imaging of glutamate dynamics during stressed and treatment conditions (Xie *et al.*, 2016).

### 1.4.1 Beyond iGluSnFR: PBP-based single-FP neuromodulator sensors

PBPs make great scaffolds for small molecule sensors because their large conformational change is relatively easy to translate into a change in fluorescence, offering unmatched dynamic ranges. Additionally, because PBPs are bacterial proteins, it is possible to screen out a large number of variants in bacteria. PBPs are versatile and can further be mutated to bind neurotransmitters for which there are no available PBPs. In addition to iGluSnFR, we and other labs are currently creating other

neurotransmitter and neuromodulator sensors based on PBP scaffolds (Kazemipour *et al.*, 2018; Looger *et al.*, 2018; Shivange *et al.*, 2019).

## 1.5 Practical considerations for choosing the most appropriate sensor

For end users, choosing the most appropriate sensor at the start of a project is paramount. The sensor selection should take into consideration technical experimental conditions such as light source, image acquisition method (one-photon, fiber photometry, two-photon, etc.), camera, image analysis algorithms, etc. as well as biological conditions such as expected ligand concentrations and the model organism or cell type. To maximize the signal to noise ratio (SNR), the intrinsic properties of a sensor such as expression, affinity, and dynamic range need to match with the time-course, frequency and concentration of release events in the brain region. Here we discuss, and summarize in Table 1.2, several practical criteria that users may wish to consider, including the properties of the sensor relative to the experimental parameters, and the potential for off-target effects.

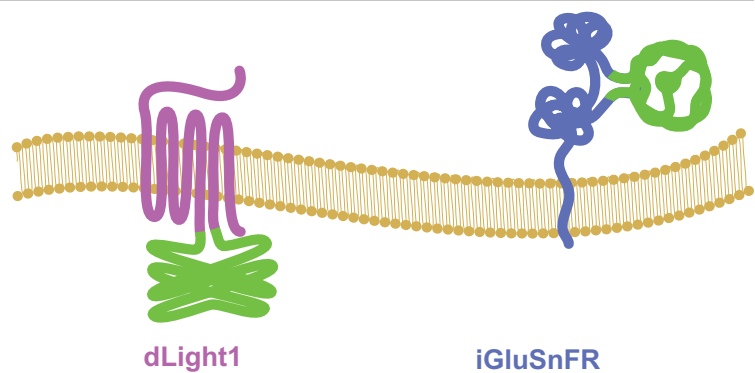
### 1.5.1 Affinity

In order to create sensors with affinities well within the physiological range, GPCR-based scaffolds are an obvious choice, in that they leverage the evolutionary specificity for the ligand of choice. In addition, there exists an array of naturally occurring GPCRs for each ligand, providing the possibility of creating multiple sensors with different affinities, such as dLight1.1-5, all produced from different receptors and with different affinities for DA.

While some PBP-based sensors, such as iGluSnFR, are able to take advantage of evolutionarily designed binding proteins, for the most part neurotransmitters do not exist in bacteria and therefore binding must be engineered into the sensor. Changing the specificity of the binding pocket is an extremely difficult process and one for which techniques need to be refined.

GPCRs have affinities that range from pM to  $\mu$ M. However, a high affinity may be a double-edged sword. While one can be sure the affinity is within the physiological range, there is the distinct possibility of the sensor buffering the ligand concentration and thus altering the properties of the cell. On the other hand, PBP-based sensors have affinities for their ligands that are in the  $\mu$ M range, which is likely to be higher than the local concentration. Thus, it is informative to determine a “sweet spot” at which the expression level maximizes the SNR while minimizing the buffering effect.

Table 1.2



Properties of the sensor		(including ultrafast and affinity variants)
Apparent affinity	100nM–1μM	0.6–53μM
Temporal dynamics	10 ms on, 100 ms off	1 ms on, 2–30 ms off
In vivo expression and activity		
Genetically encoded	Yes	Yes
Model organisms	mouse (... thus far)	mouse (knock-in), fly, fish
Subcellular localization	Obligate transmembrane protein Can be targeted to dendrite or axon	Can be tagged to any compartment
Agonist/Antagonist	Mimics endogenous receptor	Specificity is distinct from endogenous receptors
Downstream signaling	Tested negative for cAMP	No known activity in eukaryotic cells
Buffering of ligand	Potential concern	Kd outside of physiologic range reduces the potential for ligand buffering

1.5.2 Dynamic range

The dynamic range is calculated as the change in fluorescence after ligand addition divided by the fluorescence before ligand addition. Given this, it is possible to improve the dynamic range by either increasing the change in fluorescence, or by decreasing the basal fluorescence. For some applications, it is advantageous to have a very low basal fluorescence, such as photometry, where small signals are easier to detect when there is little or no background. In others, it is advantageous to have moderate basal fluorescence, such as when searching for infected or transfected cells amongst untransfected ones, prior to the addition of ligand. Sensor optimization is thus tailored to its intended

application. However, it is always advantageous to have a larger change in fluorescence. Signal detection above noise is easier when the signal is significantly larger than the noise.

Because the affinity of GPCR-based sensors is already optimal, most of the effort of creating the sensor is in optimizing the coupling. This is done by optimizing the cpGFP insertion site and then screening amino acid composition in the linker regions between cpGFP and scaffold proteins (Marvin *et al.*, 2011; Patriarchi *et al.*, 2018). The cpGFP is typically inserted into a loop region between two more structured areas of the protein whereby ligand binding creates a displacement between the two structures. A linker is then added such that steric hindrance from the cpGFP will not interfere with protein function and vice versa. A rigid linker will translate the motion of the binding protein well, but if it is too rigid, it may break the sensor. Similarly, a long linker will provide good separation between the two fused proteins, but if it is too long, the motion of the binding protein may not be translated to the GFP.

The other factor to consider is how much the binding protein moves. A large conformational change is easier to translate into a large dynamic range because there is then a wide range of angles to choose from for the dim and bright states of the sensor. While PBP-based sensors may have lower affinity for their ligands, this shortcoming is readily compensated for in their broad dynamic range due to their venus-fly-trap-like closure upon ligand binding.

### 1.5.3 Subcellular localization

One of the advantages of genetically encoded indicators over small molecules is the ability to target them to specific sub-cellular locations. To maximize SNR, subcellular targeting has proven to be effective in increasing the sensor's performance in subcellular compartments such as soma, axons and dendrites. For example, axon-targeted GCaMP and soma-targeted voltage indicators showed significantly increased sensitivity enabling robust SNR recordings compared to untargeted ones (Abdelfattah *et al.*, 2018; Broussard *et al.*, 2018).

Compared to GPCR-based sensors, PBP-based sensors offer more flexibility for fusion with a targeting motif (plasma membrane targeted, ER targeted, cytoplasmically expressed, etc). Because PBPs are soluble proteins, there are many fewer restrictions on where the sensor may exist within the cell. GPCRs are obligatory transmembrane proteins. However, adding targeting motifs is no guarantee that proper targeting will occur.

### 1.5.4 Off-target effects

Sensors are capable of disrupting normal biological functions in three major ways: by buffering the ligand concentration as discussed above, by initiating signal cascades, and by interfering with normal processes.

GPCRs, as endogenous receptors, are capable of initiating signaling cascades. Therefore, it is important to engineer them as inert sensors. PBPs, on the other hand, do not initiate signaling cascades in eukaryotic cells and thus no modification is necessary. However, the potential for off-target effects from foreign proteins, such as changes in electrophysiological, morphologic and circuit properties, must always be considered. Each new study must first determine if expression of the sensor is affecting the process being studied.

Any exogenously expressed protein has the potential to overwhelm protein production machinery or interfere with endogenous signaling pathways, particularly if it is overexpressed (Palmer *et al.*, 2011). Overexpression of these sensors (both PBP and GPCR) also may buffer the ligand (regardless of the affinity) or may begin binding lower affinity targets, thus disrupting circuitry properties. For example, overexpression of GCaMP (which is made from eukaryotic proteins but whose structure is more similar to that of the PBP-based sensors) has long been known to be an issue (Rose *et al.*, 2014). High expression levels of iGluSnFR or dLight1 have not been shown to create any gross morphological abnormalities, and bright cells respond similarly to dim cells (Marvin *et al.*, 2013; Patriarchi *et al.*, 2018). Also, in cells, dLight1 did not signal via G-protein signaling. We have observed, however, that punctate expression patterns occasionally emerge, and in these cases (either GPCR or PBP) the cell appears not to respond to normal stimuli. To balance all these effects, expression level should always be as low as possible while still obtaining a detectable signal. Very low expression will preclude sensor visualization and response detection due to a limited photon budget. To accomplish this, users may wish to explore multiple promoters such as synapsin, CAG or CaMKII, regulatory sequences, transduction methods (e.g. different viral serotypes, electroporation techniques, or transgenic lines) and examine expression level over time. It is also important to compare physiological properties of cells with and without sensor expression such as resting potential, membrane resistance and capacitance and signaling cascades, such as cAMP production.

## 1.6 Outlook

More often than not, the barriers to research are technical rather than intellectual. The development and application of tools such as genetically encoded indicators expand the horizons of what is even possible to explore in neuroscience.

Continued sensor development is likely to progress in the following ways: (1) refinement of the properties of existing sensors, including kinetics, affinity, specificity, and subcellular localization as defined by the individual needs of the user, (2) expansion of the colors available for each tool, (3) expansion of the molecular targets of sensors, and (4) adaptation of the sensors for different model organisms and experimental platforms. We and other labs are actively engaged in all four of these areas: we are refining the subcellular localization of iGluSnFR, while others are adjusting the kinetics; we and other labs are developing red and far red versions of our existing sensors; we and other labs are expanding our GPCR- and PBP-based sensors to recognize other neuromodulators and small molecule peptides (Feng *et al.*, 2018; Jing *et al.*, 2018; Sun *et al.*, 2018); and we are creating stable cell lines while other labs and organizations are making worms, fish, flies and mice that conditionally express sensors.

The application of these new sensors to existing questions in neuroscience can be potentially transformative. We and other labs devoted to tool development are working to enable this expansion and ultimately gain a deeper understanding of the brain.

## Acknowledgments

This work was supported by funding to L.T. (BRAIN Initiative U01NS090604 and U01NS013522, DP2MH107056 and R21NS095325 from the National Institutes of Health), to G.M. (ARCS Scholarship) and E.U. (Mistletoe Research Fellowship).

## References

- Abdelfattah AS *et al.* (2018) Bright and photostable chemigenetic indicators for extended *in vivo* voltage imaging. *bioRxiv*, 436840.
- Broussard GJ, Liang R, Tian L (2014a) Monitoring activity in neural circuits with genetically encoded indicators. *Front Mol Neurosci*, 7: 97.
- Broussard GJ, Liang Y, Fridman M, Unger EK, Meng G, Xiao X, Ji N, Petreanu L, Tian L (2018) *In vivo* measurement of afferent activity with axon-specific calcium imaging. *Nat Neurosci*, 21: 1272–1280.
- Corre J, van Zessen R, Loureiro M, Patriarchi T, Tian L, Pascoli V, Lüscher C (2018) Dopamine neurons projecting to medial shell of the nucleus accumbens drive heroin reinforcement Monteggia LM, Dulac C, Wolf ME, eds. *eLife*, 7: e39945.
- de Jong JW, Afjei SA, Pollak Dorocic I, Peck JR, Liu C, Kim CK, Tian L, Deisseroth K, Lammel S (2019) A neural circuit mechanism for encoding aversive stimuli in the mesolimbic dopamine system. *Neuron*, 101:133–151.e7.
- Dwyer MA, Hellinga HW (2004) Periplasmic binding proteins: a versatile superfamily for protein engineering. *Curr Opin Struct Biol*, 14: 495–504.



- Feng J, Zhang C, Lischinsky J, Jing M, Zhou J, Wang H, Zhang Y, Dong A, Wu Z, Wu H, Chen W, Zhang P, Zou J, Hires A, Zhu J, Cui G, Lin D, Du J, Li Y (2018) A genetically encoded fluorescent sensor for rapid and specific *in vivo* detection of norepinephrine. *bioRxiv*, 449546.
- Helassa N, Dürst CD, Coates C, Kerruth S, Arif U, Schulze C, Wiegert JS, Geeves M, Oertner TG, Török K (2018) Ultrafast glutamate sensors resolve high-frequency release at Schaffer collateral synapses. *PNAS*, 115: 5594–5599.
- Jing M *et al.* (2018) A genetically encoded fluorescent acetylcholine indicator for *in vitro* and *in vivo* studies. *Nat Biotechnol*, 36: 726–737.
- Kazemipour A, Novak O, Flickinger D, Marvin JS, King J, Borden P, Druckmann S, Svoboda K, Looger LL, Podgorski K (2018) Kilohertz frame-rate two-photon tomography. *bioRxiv*, 357269.
- Lin MZ, Schnitzer MJ (2016) Genetically encoded indicators of neuronal activity. *Nat Neurosci*, 19: 1142–1153.
- Looger LL, Marvin JS, Shimoda Y, Magloire V, Leite M, Kawashima T, Jensen TP, Knott EL, Novak O, Podgorski K, Leidenheimer NJ, Rusakov DA, Ahrens MB, Kullmann DM (2018) A genetically encoded fluorescent sensor for *in vivo* imaging of GABA. *bioRxiv*, 322578.
- Marvin JS *et al.* (2018) Stability, affinity, and chromatic variants of the glutamate sensor iGluSnFR. *Nat Methods*, 15: 936.
- Marvin JS, Borghuis BG, Tian L, Cichon J, Harnett MT, Akerboom J, Gordus A, Renninger SL, Chen T-W, Bargmann CI, Orger MB, Schreiter ER, Demb JB, Gan W-B, Hires SA, Looger LL (2013) An optimized fluorescent probe for visualizing glutamate neurotransmission. *Nat Methods*, 10: 162–170.
- Marvin JS, Schreiter ER, Echevarría IM, Looger LL (2011) A genetically encoded, high-signal-to-noise maltose sensor. *Proteins*, 79: 3025–3036.
- Palmer AE, Qin Y, Park JG, McCombs JE (2011) Design and application of genetically encoded biosensors. *Trends Biotechnol*, 29: 144–152.
- Patriarchi T, Cho JR, Merten K, Howe MW, Marley A, Xiong W-H, Folk RW, Broussard GJ, Liang R, Jang MJ, Zhong H, Dombeck D, Zastrow M von, Nimmerjahn A, Gradinaru V, Williams JT, Tian L (2018) Ultrafast neuronal imaging of dopamine dynamics with designed genetically encoded sensors. *Science*, eaat4422.
- Piston DW, Kremers G-J (2007) Fluorescent protein FRET: the good, the bad and the ugly. *Trends Biochem Sci*, 32: 407–414.
- Rose T, Goltstein PM, Portugues R, Griesbeck O (2014) Putting a finishing touch on GECIs. *Front Mol Neurosci*, 7: 88.
- Shivange AV, Borden PM, Muthusamy AK, Nichols AL, Bera K, Bao H, Bishara I, Jeon J, Mulcahy MJ, Cohen B, O'Riordan SL, Kim C, Dougherty DA, Chapman ER, Marvin JS, Looger LL, Lester HA (2019) Determining the pharmacokinetics of nicotinic drugs in the endoplasmic reticulum using biosensors. *The Journal of General Physiology*;jgp.201812201.
- Sun F *et al.* (2018) A genetically encoded fluorescent sensor enables rapid and specific detection of dopamine in flies, fish, and mice. *Cell*, 174: 481–496.e19.

- Tian L, Hires SA, Mao T, Huber D, Chiappe ME, Chalasani SH, Petreanu L, Akerboom J, McKinney SA, Schreiter ER, Bargmann CI, Jayaraman V, Svoboda K, Looger LL (2009) Imaging neural activity in worms, flies and mice with improved GCaMP calcium indicators. *Nat Methods*, 6:875–881.
- Xie Y, Chan AW, McGirr A, Xue S, Xiao D, Zeng H, Murphy TH (2016) Resolution of high-frequency mesoscale intracortical maps using the genetically encoded glutamate sensor iGluSnFR. *J Neurosci*, 36: 1261–1272.
- Yorgason JT, Zeppenfeld DM, Williams JT (2017) Cholinergic interneurons underlie spontaneous dopamine release in nucleus accumbens. *J Neurosci*, 37: 2086–2096.